ORIGINAL ARTICLE

lajss.org© Latin American Journal of Solids and Structures

www.lajss.org

Optimizing stiffness and lightweight design of composite monocoque sandwich structure for electric heavy quadricycle

Thonn Homsnit[a], Suphanut Kongwat[a,b]*, Kitchanon Ruangjirakit[a,b], Paphatsorn Noykanna[a], Thittipat Thuengsuk[a], Pattaramon Jongpradist[a,b]

[a]Department of Mechanical Engineering, Faculty of Engineering, King Mongkut's University of Technology Thonburi, Bangkok, Thailand, 10140. Email: thonn.homs@kmutt.ac.th, praphatsorn20404som@gmail.com, phatcharapha08@gmail.com
[b]Future Automotive Structure Research Group (FASt), Mobility and Vehicle Technology Research Center, King Mongkut's University of Technology Thonburi, Bangkok, Thailand, 10140. Email: suphanut.kon@kmutt.ac.th, kitchanon.rua@kmutt.ac.th, pattaramon.tan@kmutt.ac.th

* Corresponding author

https://doi.org/10.1590/1679-78257537

Abstract

The lightweight design of electric heavy quadricycle (L7e) vehicles has contributed to energy savings and sustainable mobility. This study proposes an optimization methodology to design a monocoque sandwich structure under operating conditions for an L7e using a finite element model via HyperWorks. Woven fiberglass fabrics and high-density PVC foam are assigned as the face and core to construct the sandwich structure, respectively. Free-size optimization based on weight minimization is applied to obtain the suitable initial thickness of face and core structures in all components. Multi-objective size optimization is then performed by minimizing both mass and material cost to determine the optimal thickness of each layer. Finally, shuffle optimization is used to modify the stacking sequence for each component to maximize structural stiffness. The results indicate that the core thickness in the passenger compartment is sufficient to maintain stiffness while maintaining the structure's lightweight. However, shuffle optimization is insignificant for the current monocoque model, as the structural stiffness is only marginally improved after the process. Additionally, this study examines the optimized models for structural stiffness and discusses suitable procedures for designing a lightweight and safe electric vehicle.

Keywords

Heavy quadricycle; lightweight design; monocoque sandwich structure; composite materials; structural optimization

Graphical Abstract

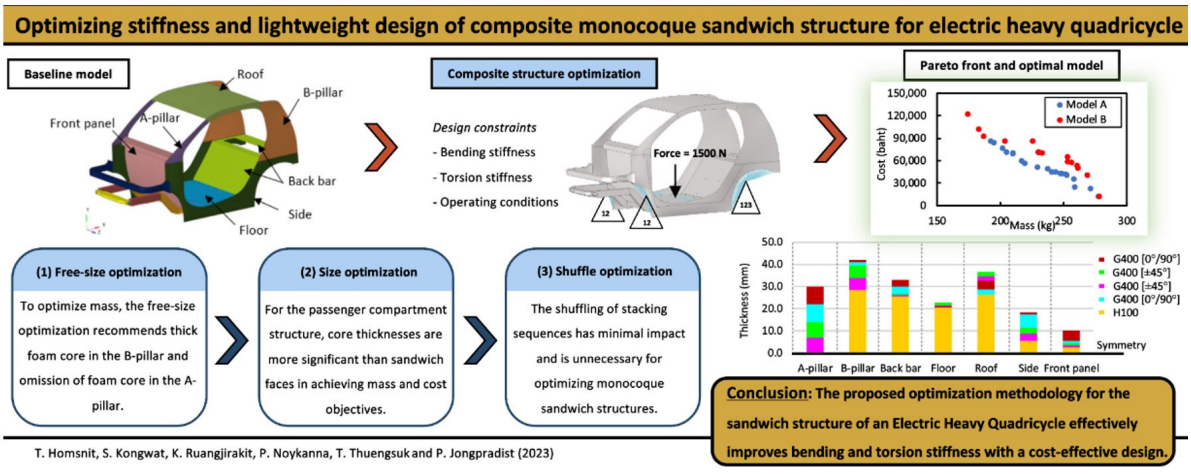

Received: February 27, 2023. In revised form: March 08, 2023. Accepted: April 03, 2023. Available online: April 05, 2023.
https://doi.org/10.1590/1679-78257537

1 INTRODUCTION

The global use of electric cars rapidly grows due to consumer need for cost-efficient and environment-friendly cars (Ewert, Brost, Eisenmann, & Stieler, 2020). Electric heavy quadricycle classified by the European Union as a mini fuel-efficient vehicle as L7e is an alternative for electric vehicles (EV) majorly used in urban areas for local transportation (Kongwat et al., 2021). The specifications of L7e typically provide that the vehicle's unladen weight, excluding other components, must not exceed 450 kg for the transport of passengers. The lightweight design and low carbon footprint are prominent elements of the L7e. Nonetheless, the structural strengths of the L7e require considerable improvement since the overall dimensions are smaller and there are fewer regulations for the safety of L7e than conventional passenger cars (Kongwat et al., 2022; Redelbach et al., 2014; Wüstenhagen et al., 2021). Thus, it is crucial that a structurally stiff and safe design is developed to improve the overall performance of the L7e.

A lightweight structural design can be achieved by several approaches, such as modifying the shape of the structural frame and components and replacing the conventional materials with high-performance materials (Denny et al., 2018). Optimization procedures are generally employed to efficiently design the structural body shape or frame for various vehicle types and applications (Cavazzuti et al., 2011; Kim et al., 2018; Kongwat and Hasegawa, 2020; Patel et al., 2009; Sudin et al., 2014). Kongwat et al. (2020) designed an automotive body frame under normal operation conditions and rollover safety using topology and size optimizations. Similarly, Kunakorn-ong and Jongpradist (2020) applied the optimization methodology based on the response surface method (RSM) when seeking to design a vehicle structure optimally. These studies present optimistic methods to develop lightweight designs. However, the procedures utilized were rather complex due to the structural models being iteratively re-designed. Thus, a design by substituting each structural component's material with lightweight materials, particularly composite materials, could readily improve structural performance (Czerwinski, 2021; Kunakorn-ong et al., 2020).

Composite materials and sandwich structures are widely utilized in the design of engineering structures, notably in the aircraft and automotive industries (Gheorghe et al., 2021; Patel et al., 2018; Sinha et al., 2021; Tranchard et al., 2015), to obtain weight reduction and gain a high stiffness-to-weight ratio (Meyers, 2002). Additionally, a composite monocoque structure can enhance performance in lightweight automotive vehicles (Wu et al., 2014). Previous research showed that using carbon-fiber composite monocoque structures for three-wheeled and formula-style vehicles could accomplish a high strength-to-weight ratio under desired conditions with low fuel consumption (Hiller, 2020; Messana et al., 2019). A sandwich structure consisting of two thin but stiff skins and one thick core could also be an excellent option for implementing the monocoque design to improve its performance further. The core material typically has a lower strength and density with a large thickness to resist bending deformation (Hoff, 1986). Various skin and core materials, such as syntactic foams, honeycombs, and carbon fiber, have been studied to investigate their characteristics and strengths (Reddy et al., 2016; Story, 2014; Ugale et al., 2013). Furthermore, an optimal thickness of the skin and core influences the stiffness and weight, which is suitable for each engineering application and loading condition.

In the design of automotive structures, the requirements commonly include stiffness requirements, i.e., bending stiffness and torsion stiffness, and safety factor under normal operating conditions (Ary et al., 2021; Li & Feng, 2020; Singh, 2010). Ary et al. (2021) analyzed the shell eco-marathon structure with variations of materials and thicknesses under normal conditions, such as longitudinal and lateral loadings from braking and cornering. A suitable model was obtained by seeking the maximum torsional strength similar to the process used in designing an automobile chassis (Santa Rao et al., 2016). Kunakorn-ong et al. (2020) employed finite element analysis to optimize an electric bus body using a monocoque sandwich structure under driving conditions, stiffness requirements, and natural frequency. The new structure reduced the structural weight by 63.3% from the baseline. Although advanced materials such as composites can significantly improve bending and torsion stiffness, the material and manufacturing costs are considerably higher than the conventional materials (Ciampaglia et al., 2021). Optimization methodology to obtain an optimal model in which the structural strength and cost are considered as the objective functions through the design procedure. Velea et al. (2014) developed and implemented optimization procedures using both single and multi-objective functions to design an FRP sandwich body of an electric vehicle, in which the structural performance was optimized concerning the weight, material cost, and global and local stiffness. Thus, optimization procedures are beneficial when multiple objectives need to be simultaneously considered.

This research aims to design a sandwich monocoque structure for an L7e vehicle and implement the techniques in free-size, size, and shuffle optimization to attain the stiffness requirements and lightweight. The loadings under driving conditions, i.e., bending stiffness, torsion stiffness, lateral load, and longitudinal load, are concurrently evaluated in the optimization problem. Finite element analyses are utilized to investigate the body strength and optimal solution via HyperWorks. Both single and multi-objective optimizations are performed to achieve a suitable sandwich panel thickness for each structural component. All compromise solutions from the multi-objective optimization are compared through the acquired Pareto-frontiers. Finally, the most practical solutions are examined according to the significance of the objectives.

2 STRENGTH REQUIREMENTS FOR THE MONOCOQUE DESIGN

An optimization procedure generally requires design constraints as criteria to acquire an optimal solution. This research is concerned with designing a monocoque structure for an L7e based on normal operating conditions defined in the optimization constraints: bending stiffness; torsion stiffness; and lateral and longitudinal loadings.

2.1 Bending stiffness

Bending stiffness indicates the ability of a structure to carry the self-weight load and other components such as a battery, passenger, motor, and control box (Malen, 2011). The bending stiffness (K_b) of the structure is calculated using Equation (1), where F_y is the force that vertically applies along the vehicle structure and δ_y represents the maximum displacement measured in the direction of applied loading.

$$K_b = \frac{F_y}{\delta_y} \tag{1}$$

Bending stiffness can be divided into two types to consider the strength of the monocoque structure: pure bending and combined bending. Pure bending is evaluated when the bending load is directly applied to the structure, and the stiffness is calculated by using Equation (1). Meanwhile, the combined bending condition measures the body stiffness when loads from other components are included. It is used to determine the safety factor (SF) to ensure the body performance under bending by using Equation (2), where σ_{all} is allowable stress and σ_c is the maximum composite stress which seeks on each layer.

$$S.F. = \frac{\sigma_{all}}{\sigma_c} \tag{2}$$

2.2 Torsion stiffness

Torsion stiffness (K_t) measures the structural ability to withstand loading when a vehicle wheel falls into a pothole while traveling on an uneven road without permanent deformation. The torsion stiffness can also be classified as pure torsion and combined torsion. Pure torsion is indicated by the resistance of the body offered per degree of change in angle when twisted from the applied coupling forces (Kongwat et al., 2020). Equation (3) is used to compute the structural stiffness from pure torsion, where T is the applied torque in the front shaft axis, R is the distance between the wheel hubs, and z_1 and z_2 are deflections on the left and right sides of the shaft axis.

$$K_t = \frac{T}{\tan^{-1}\left(\frac{z_1 + z_2}{R}\right)} \tag{3}$$

The combined torsion represents the structural ability to resist deforming from twisting loads with the whole body, which takes the reaction force and other component loads into account and evaluates the stiffness using the safety factor in Equation (2) as the criteria.

2.3 Lateral and longitudinal loading

Lateral and longitudinal conditions represent the ability to resist plastic deformation when a vehicle turns left or right and decelerates from braking (Malen, 2011). The safety factors under these conditions are also measured using Equation (2) to classify the strength of the L7e body. The monocoque structure needs to pass all strength requirements during the design process.

3 VALIDATION OF THE COMPOSITE MATERIAL MODEL

Anisotropic woven glass fiber composite is applied to design the monocoque structure of L7e. In finite element analysis, the material model and its properties are necessarily validated and verified to ensure the characteristics of each

direction through the simulation procedure. The conditions of the drop weight impact test are set according to the ASTM-D7136 standard (Akangah & Shivakumar, 2013), as shown in Figure 1. Simulation results are obtained by using the Radioss solver and validated with the experiment (Jongpradist et al., 2022).

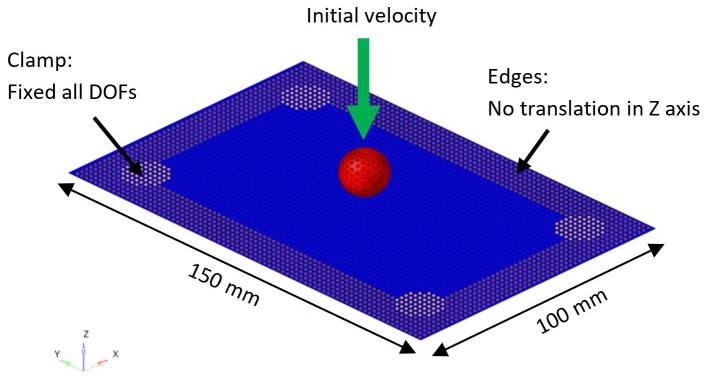

Figure 1 Boundary conditions for the drop weight impact test.

The FE model in Figure 1 consists of a composite plate and an impactor. The composite rectangular plate is created as a deformable body 150 mm long and 100 mm wide. The plate is discretized into 4-node quadrilateral elements with an element size of 2 mm consisting of 3,876 nodes and 3,750 elements. The composite plate comprises a 14-layer woven glass fabric with a surface density of 400 g/m^2 (G400). The stacking sequence is [G(0°/90°)$_6$/(±45°)$_8$], and the ply thickness for each layer is 0.4 mm. The material properties of G400 are listed in Table 1 (Jongpradist et al., 2022), and the Tsai-Wu criteria (Groenwold & Haftka, 2006) available for MAT25 (COMPSH) in Radioss is used to investigate the characteristics of material plasticity. The impactor is in a spherical shape of 16-mm diameter created by using solid elements with a mass of 9.6 kg and is assigned as a rigid body. The impactor's initial velocity is applied downward (-Z-direction) according to the testing condition for each impact energy. Furthermore, the surface-to-surface contact type is defined at the contact surfaces between the impactor and composite plate.

Table 1 Material properties of the sandwich structure (Jongpradist et al., 2022).

Material Properties	G400	H100 Foam
Longitudinal modulus [E_1] (MPa)	18,036	105
Transverse modulus [E_2] (MPa)	18,036	105
In-plane shear modulus [G_{12}] (MPa)	2,219	2,212
Longitudinal tensile Strength [X_t] (MPa)	415	411.4
Longitudinal compressive strength [X_c] (MPa)	200	370.6
Transverse tensile strength [Y_t] (MPa)	415	411.4
Transverse compressive strength [Y_c] (MPa)	200	370.6
In-plane shear strength [S] (MPa)	75	105
Mass density [ρ] (kg/m^3)	1,588	1,336
Poisson's ratio	0.1	0.05

The validation procedure compares the force-displacement results between the experiments from Jongpradist et al. (2022) and the FE model under three cases of impact energy: 50, 75, and 90 Joules. The force-displacement curves' results are compared and shown to provide a similar trend for all cases, as exemplified by the 50-Joule impact energy in Figure 2. Additionally, the maximum forces and the maximum displacements are slightly different from the experiments, as summarized in Table 2. Errors from the experiment could occur from the measurement method, data collected from sensors, and noise from devices during the test. However, it can be confirmed that the simulation procedure of composite material is sufficiently accurate for further analysis and design of the L7e monocoque structure.

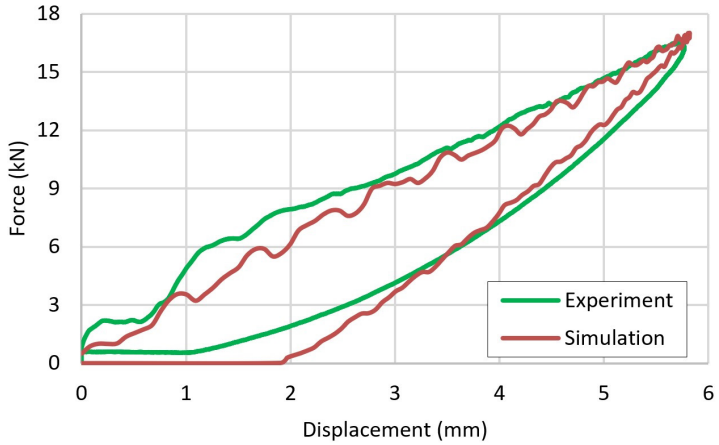

Figure 2 Comparison of experimental and simulation results from the drop weight impact test with an impact energy of 50 J.

Table 2 Comparison between the experiment (Jongpradist et al., 2022) and simulation results.

Energy (J)	Maximum force (kN)			Maximum displacement (mm)		
	Experiment	Simulation	Error (%)	Experiment	Simulation	Error (%)
50	16.32	17.01	**4.21**	5.79	5.82	**0.46**
75	19.41	21.02	**8.29**	7.37	7.55	**2.40**
90	21.77	24.53	**12.68**	7.65	7.71	**0.78**

4 FINITE ELEMENT MODEL OF THE MONOCOQUE STRUCTURE

This work focuses on designing a monocoque structure for two-seated L7e under desired loading conditions, using optimization procedures via a finite element model. The overall dimensions of the L7e frame are 1.2 m wide, 2.5 m long, and 1.4 m high. The L7e model consisting of two main parts, the passenger compartment, and frontal structures, is presented in Figure 3. The compartment area includes seven parts, i.e., the sub-structure, floor, roof, back bar, A-pillars, B-pillars, side, and front panel, while the frontal structure contains four parts of the upper beam, lower beam, front rails, and crash boxes. The L7e model is discretized by mixing the 3-node triangular and 4-node quadrilateral shell element types. Each node has 6 degrees of freedom (3 translations and 3 rotations). The L7e model consists of 61,708 nodes and 62,688 elements, and the maximum element size is 10 mm. In addition, the weight of the structural components, i.e., seats, passengers, battery, motor, and control box, are assigned by using distributed forces on those areas, with the respective weights presented in Table 3.

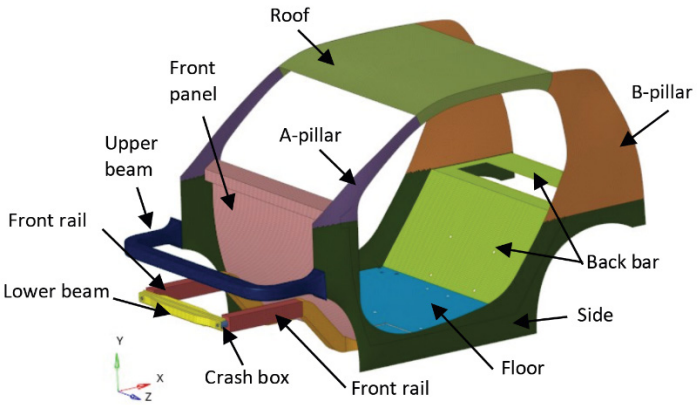

Figure 3 Finite element model of the monocoque structure for L7e.

Kongwat et al. (2022) conducted a comprehensive study and analysis of the L7e baseline model, with a primary focus on the use of steel as the structural component. The stiffness values for the baseline model were also evaluated, with results showing 4,655 N.m and 15,528 N.m/deg for bending and torsion cases, respectively. Additionally, the structural mass of the model was measured to be 375 kg.

Table 3 Weight of components for the L7e model.

Components	Weight (kg)	Force (N)
Passenger and seat	93.7	919.2
Battery	350.0	3,433.5
Motor	50.0	490.5
Control box	15.0	147.2

4.1 Loading conditions for bending stiffness

Pure bending stiffness is analyzed by applying 1,500 N of the force at the center of the left and right sides (Figure 4a), representing a bending load placed upon the L7e structure. The constraints are defined at both the front and rear wheels to take the bending deformation of the body frame (Fang and Kefei, 2019). Figure 4b illustrates the loading condition to analyze the safety under bending and combined bending stiffness. The weights of additional components not included in the FE model are bound by the RBE3 element in HyperWorks and applied to the L7e structure along with the gravitation load.

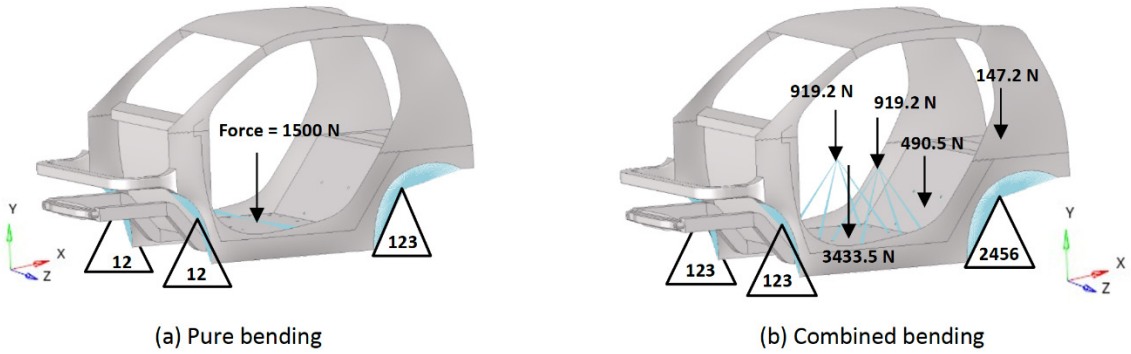

(a) Pure bending (b) Combined bending

Figure 4 Loadings and boundary conditions for bending stiffness.

4.2 Loading conditions for torsion stiffness

Structural deformation from the pure torsion case occurs when couple forces of 2,000 N are applied to the left and right front wheels (Figure 5a) while the rear wheels are constrained in all translational directions (Fang and Kefei, 2019). In the case of combined torsion load representing the occasion that the left front wheel falls into a pothole, the force twice the total body weight is applied to the left front wheel, whereas the other wheels are constrained (Chen et al., 2015) (Figure 5b). The mass of the other components is also considered to analyze the safety under the combined torsion case.

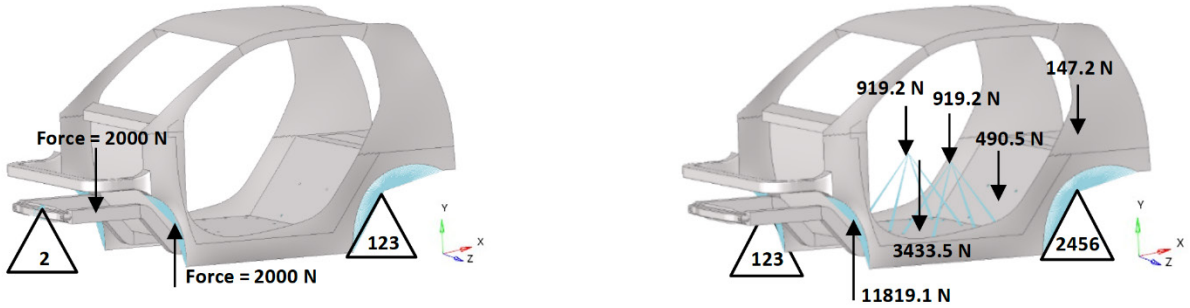

(a) Pure torsion (b) Combined torsion

Figure 5 Loadings and boundary conditions for torsion stiffness.

4.3 Loading conditions for lateral and longitudinal cases

Longitudinal loading simulates the structural behavior of the L7e body when the car brakes or decelerates, while lateral loading is concerned with the condition when the vehicle turns left or right. The constraints of these cases are

displayed in Figure 6. The external forces occur to the structure under these circumstances are assigned using the dynamic factors of 1.5g in the longitudinal direction and 2g in the lateral direction (Chen et al., 2015).

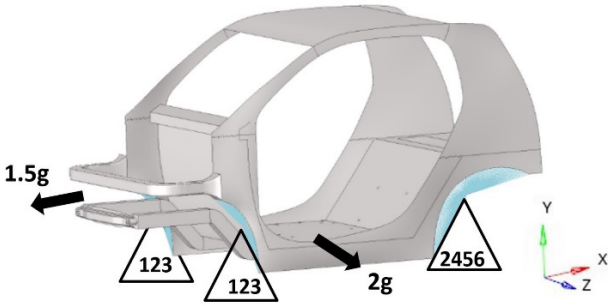

Figure 6 Loadings and boundary conditions for lateral and longitudinal cases.

5 OPTIMIZATION METHODOLOGY AND RESULTS

This work proposes three steps to optimize the composite monocoque structure for L7e: free-size, size, and shuffle optimization. The overall methodology is illustrated in Figure 7, in which the free-size optimization is first employed to preliminary investigate a suitable material for each component. Then, the layout configuration is redefined for each structural component based on the result interpretation. The size optimization is then used to determine the required thickness of each ply according to the design constraints. Finally, shuffle optimization is sought for the best stacking sequence on each structural part. According to the proposed processes in the current study, multi-objective optimization is performed to establish the optimal results only in the size optimization procedure, while the other processes are optimized based on single-objective problems.

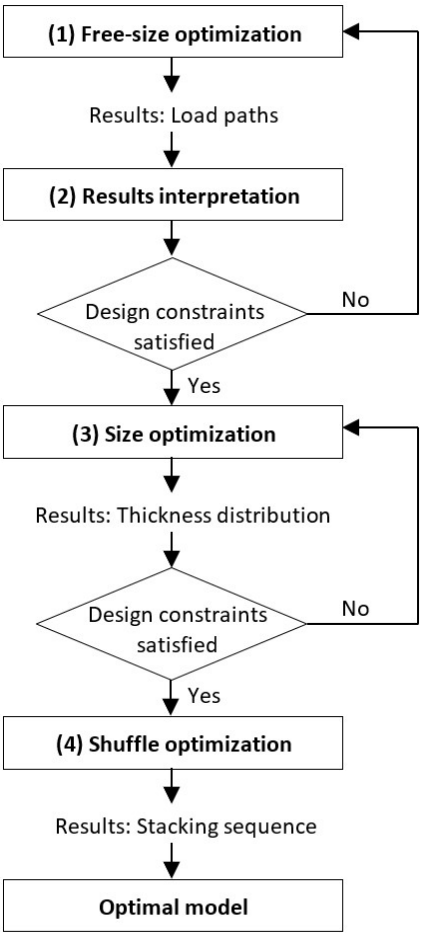

Figure 7 An optimization methodology for a monocoque sandwich structure.

5.1 Free-size optimization

Free-size optimization is initially performed to determine the suitable thickness and ply configuration for each component under the desired objective function and constraints. This method applies the concept of super-plies to seek a thickness distribution for each fiber orientation when all conditions meet the requirements. An ideal conceptual design can be quickly generated from free-size optimization results to determine the number of fiber orientations, the maximum thickness of each orientation, and the total laminate thickness. In this current work, free-size optimization is implemented by using the Optistruct solver.

The initial L7e model for free-size optimization defines the sandwich structure consisting of 8 layers along the height with the stacking sequence, as illustrated in Figure 8. The G400 woven glass fabrics with fiber orientation in 0°/90° and ±45° are used as the face of the sandwich structure. The core material is high-density PVC foam at 100 g/m^3 (DIAB Divinycell H100 Foam). The material properties for both face and core structures are presented in Table 1. In this step, two models of the L7e with different thicknesses for each layer are considered, as listed in Table 4. Model A and model B are primarily assigned as a quasi-isotropic laminate with the same thickness of 0°/90° and ±45° layers. The total thickness for both models is equal to 70 mm. Finally, the optimal L7e model will be selected based on the highest structural performance that satisfies all optimization objectives and constraints.

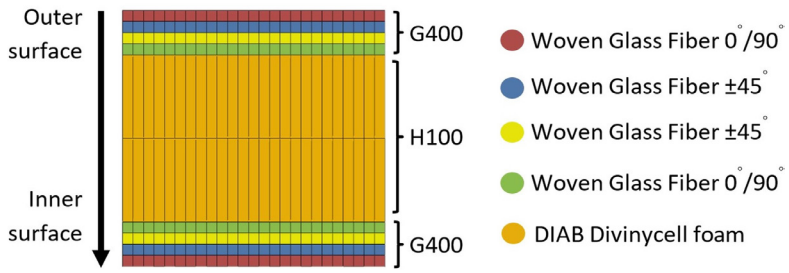

Figure 8 The initial section of the composite sandwich body.

Table 4 Geometry of the initial L7e models for size optimization.

Models	Thickness in each layer orientation (mm)		
	Face (G400)		Core (H100)
	0°/90°	±45°	
Model A	5	5	15
Model B	3.75	3.75	20

5.1.1 Free-size optimization problem

The thicknesses of both face and core materials in each component are separately defined as the design variables for the free-size optimization, aiming to minimize the overall structural mass. Since the section of the sandwich structure (Figure 8) is symmetrically defined, the design variables are then considered by using only half of the total cross-sectional thickness. The optimization constraints concern normal operation conditions to improve the structural stiffness and safety factors, as shown in Table 5. The parameter $K_{b,baseline}$ and $K_{t,baseline}$ denotes the bending and torsion stiffness of the L7e baseline model. The maximum face thickness (x_{ij}) and the maximum core thickness (y_j) are specified as 20 mm and 30 mm, respectively. In addition, the total thickness of each structural component must not exceed 70 mm. In summary, the mathematical formulation for free-size optimization can be expressed by Equations 4a, 4b, and 4c, as shown below.

$$\text{Design variables: } \begin{cases} X = \{x_{11}, \ldots x_{ij}\} \\ Y = \{y_1, \ldots y_j\} \end{cases} \tag{4a}$$

$$\text{Minimize: } f(X,Y) = \sum_{i=1}^{n}\sum_{j=1}^{m}\left(\rho_{ij} \times A_{face} \times x_{ij}\right) + \sum_{j=1}^{m}\left(\rho_j \times A_{core} \times y_j\right) \tag{4b}$$

$$\text{Subject to: } \begin{cases} 0.1 \le x_{ij} \le 20 \quad (mm) \\ 0.1 \le y_j \le 30 \quad (mm) \\ 0.5 \le \left(x_{ij} + y_j\right) \le 70 \quad (mm) \\ g_k(x) - g_k^U(x) \le 0 \quad where \quad k = 1,\ldots,6 \end{cases} \tag{4c}$$

where X and Y respectively denote thickness vectors of face and core. The subscript ij represents the thickness of the i^{th} layer of the j^{th} element where the number of layers within each structural component n is 4 and the number of compartment parts m is 7. Thus, the total number of design variables is 35. The function $g_k(x)$ and $g_k^U(x)$ are the k^{th} constraint response, in which the upper bound values are presented in Table 5. To optimize the L7e monocoque, the required pure bending and torsion stiffness, which defines two times the stiffness values from the baseline model, are 9,310 N/mm and 31,056 N.m/deg, respectively. The local optimal thickness is iteratively determined in each structural model. After several repetitions, an optimal thickness for all structural components for two different L7e models was obtained.

Table 5 Optimization constraint for each load case.

Indices	Load cases	Constraints
k_1	Pure bending stiffness	$K_b \geq 2K_{b,baseline}$
k_2	Pure torsion stiffness	$K_t \geq 2K_{t,baseline}$
k_3	Combined bending stiffness	$S.F. > 1.5$
k_4	Combined torsion stiffness	
k_5	Lateral loading	
k_6	Longitudinal loading	

5.1.2 Resuts from free-size optimization

The results of the free-size optimization demonstrate the thickness distributions of each fiber orientation and sandwich core for each structural component, as exemplified in Figure 9 for the optimal core thickness of the A and B-pillars. The optimization results from model A indicate that the B-pillar requires a thick core of the sandwich structure to carry the loads and increase stiffness. On the contrary, the core thickness in most areas of the A-pillar can be reduced while all optimization constraints are satisfied. Therefore, the foam core can be removed from the A-pillar section. After the result interpretations from free-size optimization, the thicknesses for fabric layers and core in each component are implemented into the models for the size-optimization procedure.

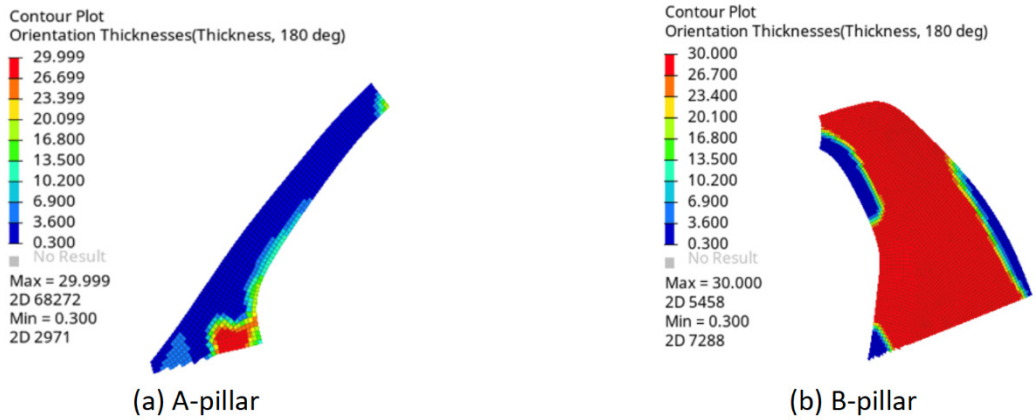

Figure 9 Core thickness distribution results from the free-size optimization.

Figure 10 summarizes the schematics of the sandwich structure for all components. The core thickness of the A-pillar is clearly distinguished from the free-size optimization results of models A and B. Additionally, model B coincidently acquires the maximum thickness of foam core for all components, while the face thickness is uniformly distributed in the optimized model B. However, both models of L7e passed all requirements for structural stiffness safety, as summarized in Table 6. The A-pillars

apparently affect the deformation resistance in the bending load more than the torsion load case. The face thickness does not significantly affect the strength of the L7e structure under normal operating conditions. Furthermore, the structure of models A and B can reduce the weight by 23.8% and 22.1%, respectively, compared with the L7e baseline model.

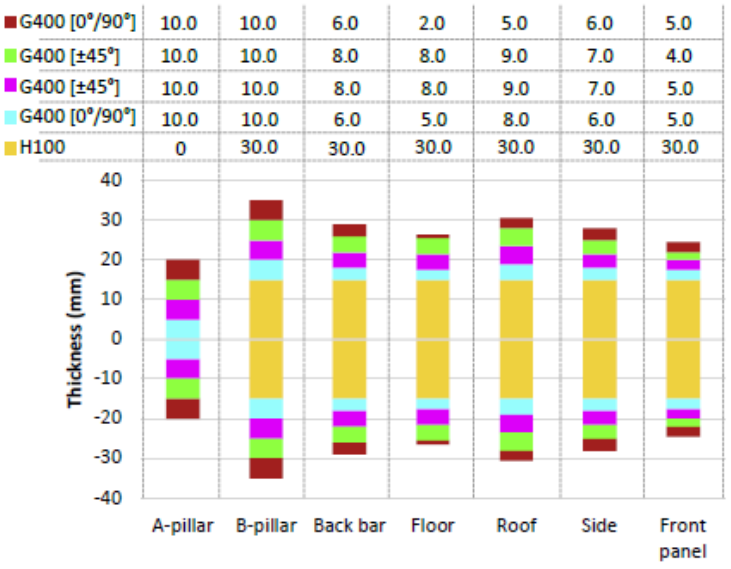

(a) Model A

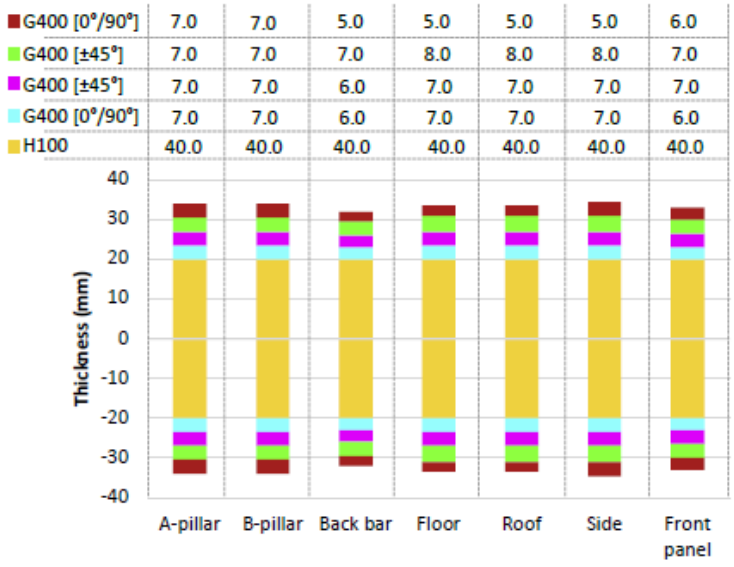

(b) Model B

Figure 10 Result interpretations from free-size optimization.

Table 6 Analysis results on the L7e models from free-size optimization.

Models	Structural mass (kg)	K_b (N/mm)	K_t (N.m/deg)	Minimum S.F.
Model A	288.4	20,548	31,495	1.67
Model B	292.3	25,000	31,114	1.72

5.2 Size optimization

An optimal thickness of each fiber orientation in each component is the primary variable to investigate during the multi-objective size optimization for the L7e models, aiming to minimize both mass and material cost. In the current work, the size optimization is performed based on the global response surface method (GRSM) implemented in HyperStudy. The GRSM seeks an optimal solution based on the concepts of an adaptive response surface, which parallelly

generates and analyses additional designs to ensure a balance for both local and global search capabilities. Additionally, the GRSM can provide accurate and efficient results by handling the optimization procedure with multi-objective formulations (Pajot, 2013).

Design variables for size optimization are the same as the free-size optimization, i.e., the thickness of each face orientation and sandwich core in all structural components as described in Equation 4a. Nonetheless, the thicknesses of the face and core are assigned with the upper bound of 8 mm and 30 mm to correspond with the previously determined thicknesses from free-size optimization, and the total thicknesses are set not exceed 40 mm. The optimization constraints are also defined by using the same equations as the free-size optimization by considering the required structural stiffness and safety factor. Therefore, the formulation for size optimization can be stated by Equation 5, where C_{face} and C_{core} are the material cost per kilogram of face and core, respectively (as shown in Table 7).

$$F=\left[f_1(X,Y), f_2(X,Y)\right]$$

$$\text{Minimize: } \begin{cases} f_1(X,Y)=\sum_{i=1}^{n}\sum_{j=1}^{m}\left(\rho_{ij}\times A_{face}\times x_{ij}\right)+\sum_{j=1}^{m}\left(\rho_j\times A_{core}\times y_j\right) \\ f_2(X,Y)=\sum_{i=1}^{n}\sum_{j=1}^{m}\left(C_{face}\times\rho_{ij}\times A_{face}\times x_{ij}\right)+\sum_{j=1}^{m}\left(C_{core}\times\rho_j\times A_{core}\times y_j\right) \end{cases} \tag{5a}$$

$$\text{Subject to: } \begin{cases} 0.1\le x_{ij}\le 8 \quad (mm) \\ 0.1\le y_j\le 30 \quad (mm) \\ 0.5\le\left(x_{ij}+y_j\right)\le 70 \quad (mm) \\ g_k(x)-g_k^U(x)\le 0 \quad where \quad k=1,\ldots,6 \end{cases} \tag{5b}$$

Table 7 Material costs per unit kg.

Indices	Materials	Unit Cost per weight (baht/kg)
C_{face}	Woven Glass Fiber (G400)	44
C_{core}	DIAB Divinycell foam (H100)	3,066

The Pareto-frontier is generally acquired from the multi-objective optimization during the iterative calculation to define a set of non-dominated solutions, in which each objective is presented with an optimal solution. Figure 11 illustrates the Pareto-frontier from the size optimization of the L7e models. The non-dominated solutions of models A and B tend to increase material costs when the structural weight is lighter. The pareto-frontier determined by using model A is more favorable because the material cost is considerably lower when the structural mass is between 200 and 270 kg. Nevertheless, only Model B can accomplish the optimized model with a structural mass of less than 190 kg.

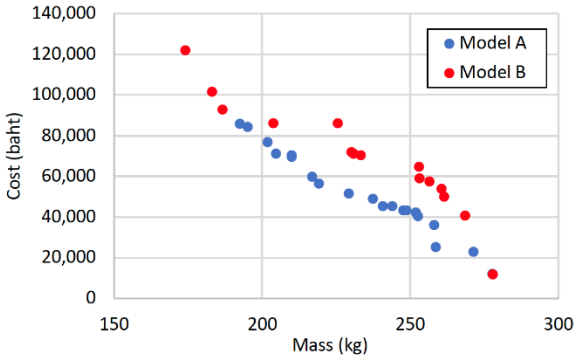

Figure 11 Pareto-frontier from size-optimization.

Moreover, the optimal results from model B show that the core thicknesses of the side panels and the front panel are diminished to minimal and the foam core is removed in the A-pillar section. Therefore, it can be deduced that the core materials of the outer components of the passenger compartments offer an inefficient effect to resist deformation

under loads from operating conditions when the material cost is also considered. This is because the stiffness of these parts contributes to the torsional stiffness of the structure rather than the bending stiffness. Moreover, when the computed model B from size optimization was reanalyzed by FE simulation, some parts could not pass the structural stiffness requirement, while the total thickness also exceeded the upper bound limit in a few parts. Thus, only model A is preferred and selected to further implement and optimize in the next step to seek an optimal stacking sequence on each component of the monocoque L7e structure.

The schematic of each component's optimal thicknesses from the size optimization of model A is displayed in Figure 12 by selecting an equal weighting factor for both objective functions. It is found that the effects of the core thicknesses in the sandwich structure of the passenger compartment (B-pillar, back bar, floor, and roof structures) to the structural stiffness are more significant than the sandwich faces in resisting deformation from payloads with the lightweight design. Consequently, the core thicknesses of the side and front panels become noticeably less than the free-size optimization. The optimized model also passed all requirements, in which the bending and torsion stiffness are respectively 13,024 N/mm and 31,200 N.m/deg. The minimum S.F. for other conditions is 1.61 when the structural weight is 195 kg and the material cost is approximately 84,000 Baht.

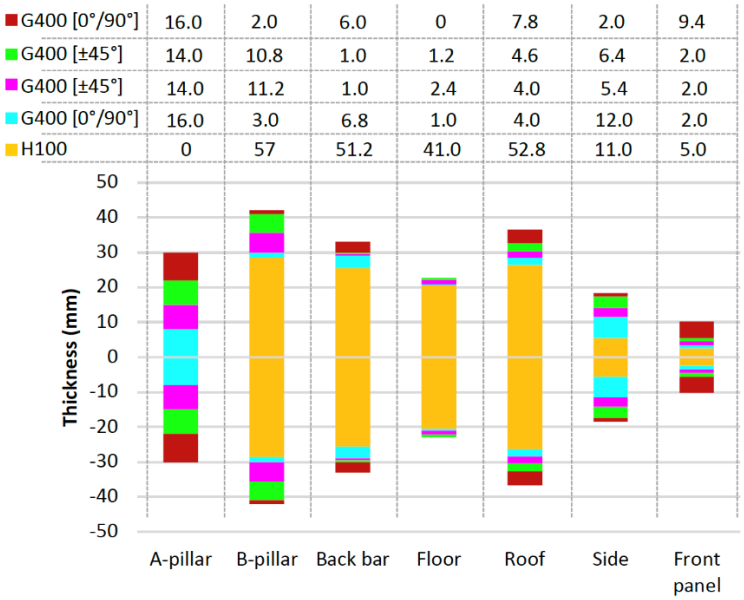

Figure 12 Schematic of optimized solutions from the size optimization.

5.3 Shuffle optimization

After the size optimization process, the face of each sandwich component of monocoque L7e structure is designed using a stacking sequence $[G(0^{\circ}/90^{\circ})_p/(\pm45^{\circ})_r/(\pm45^{\circ})_s/(0^{\circ}/90^{\circ})_q]$. The parameters p and q are the number of plies for the outer and inner layers of the $0^{\circ}/90^{\circ}$ fiber orientation, and r and s are the number of plies or the outer and inner layers of the $\pm45^{\circ}$ fiber orientation. The optimal sandwich configuration of each structural component and their thicknesses after free-size and size optimization shown in Figure 12 is next optimized for the most efficient model through shuffle optimization. This process aims to establish an optimal stacking sequence of the sandwich face for each component to minimize structural compliance under all design constraints.

After iterative calculations, the optimized stacking sequences of each component are obtained in Figure 13. The optimized model only modifies the order of the stacking sequence for each fiber orientation, while the total thicknesses and the weight of the sandwich structure are equal to the previous model from the size optimization. After applying shuffle optimization, the $\pm45^{\circ}$ layers of the floor and roof were relocated to the exterior layers, while the remaining sections maintained the $0^{\circ}/90^{\circ}$ layers on the exterior. Though, shuffling the layers of fiber orientation can somewhat increase the stiffness of the car body as expected. The optimized model resulting from shuffle optimization demonstrates an improvement in both bending and torsion stiffness. Specifically, the optimized model achieves a bending stiffness of 12,975 N/mm and a torsion stiffness of 31,474 N.m/deg. The improvement is not much realized, possibly because the core thicknesses of the sandwich structure are somewhat large and dominate the effects on structural stiffnesses. However, since the shuffle optimization process requires substantial computational resources, the process can be omitted from the current design.

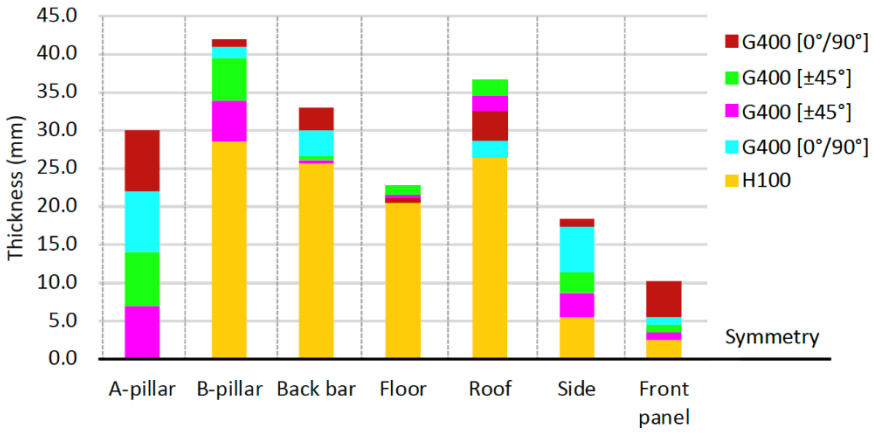

Figure 13 Schematic of optimized solutions from the shuffle optimization.

5.4 Result comparisons

The L7e monocoque model using sandwich structure is acquired from free-size, size, and shape optimization. The optimized model's total face and core thicknesses from all optimization procedures are presented and compared in Figures 14a and 14b. The free-size optimization delivers uniform core thickness for all components, except for the A-pillar, while the thicknesses of the 0°/90° and ±45° faces are different. The size optimization based on weight and cost minimization distinctly classified the thickness of core and face components by only increasing the core thickness of the passenger compartment to maintain the stiffness with a lightweight design. The foam cores used in the A-pillar, side, and front panels are necessary only to a minimal extent, as these parts primarily contribute to the torsional stiffness of the monocoque rather than the bending stiffness.

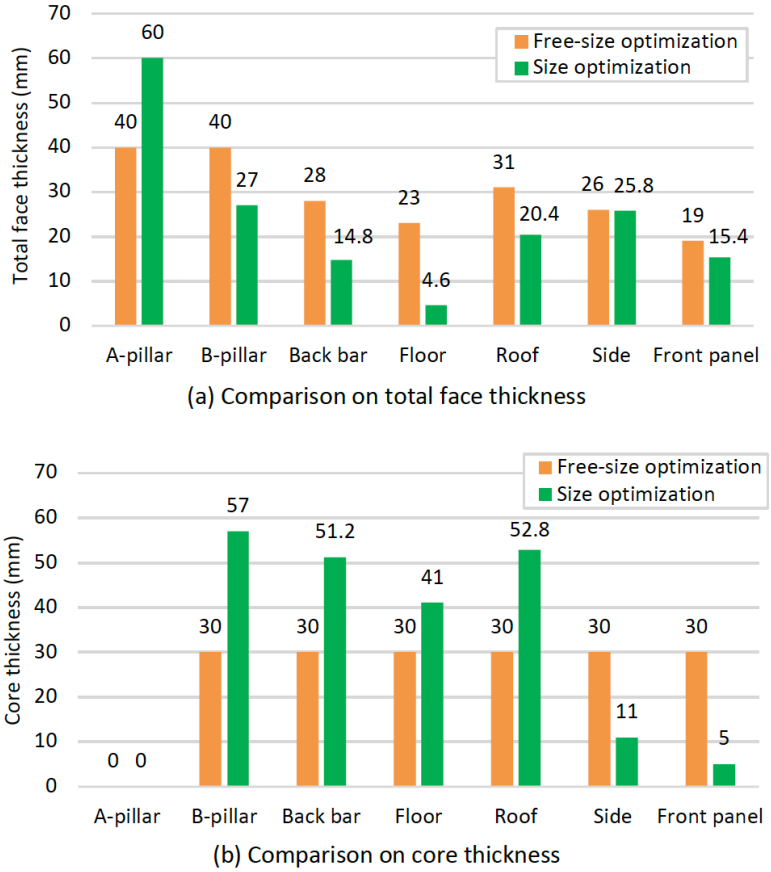

Figure 14 Thickness comparison of the optimized models from each optimization.

The bending and torsion stiffness of the different L7e models are compared in Figure 15, in which the optimized L7e models from free-size, size, and shuffle optimization are found to improve all structural strengths to pass the requirements. Comparing with the baseline model, the final optimized model increases the bending and torsion stiffness by 178.7% and 102.7%, respectively. Furthermore, the minimum safety factor was around 1.61 under the combined torsion load case when the structural weight is 195 kg, which is decreased by 48% from the baseline model.

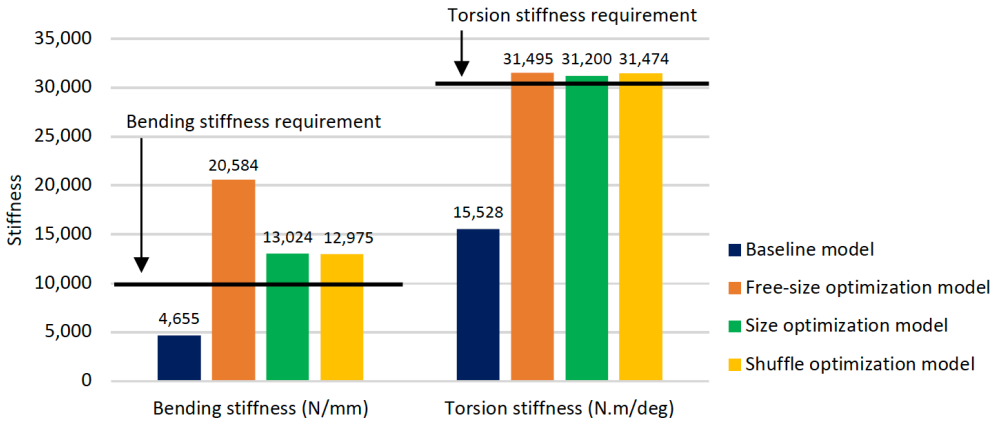

Figure 15 Comparison of bending and torsion stiffness from the different L7e models.

6 CONCLUSIONS

This study presents a comprehensive optimization methodology to design a composite sandwich structure for a heavy quadricycle's monocoque, considering various design constraints such as bending stiffness, torsion stiffness, and operating conditions. The methodology comprises free-size optimization to determine optimal material configurations, size optimization to minimize vehicle weight and cost by determining the appropriate thickness for each sandwich layer, and shuffle optimization to modify the stacking sequences of the composite faces with different fiber orientations. The analysis reveals that the compartment zone's sandwich structure significantly affects bending stiffness, while the A-pillar, side, and front panels contribute mainly to torsional stiffness with minimally required core thickness. Notably, the inclusion of shuffle optimization in the optimization procedure is unnecessary, as the obtained structural stiffness is similar to that of the optimized model from size optimization. To enhance the safety of the L7e model, future work should consider optimizing its crashworthiness as a constraint.

Acknowledgments

The authors wish to acknowledge financial support from Thailand Science Research and Innovation (TSRI) Basic Research Fund: Fiscal year 2023 under project number FRB660073/0164 (Program Sustainable Mobility) and Research Grant for New Scholar 2021 with contract number RGNS 64-101 from the Office of the Permanent Secretary, Ministry of Higher Education, Science, Research, and Innovation.

Author's Contribuitions: Conceptualization, P Noykanna, T Thuengsuk, K Ruangjirakit and S Kongwat; Methodology, P Noykanna, T Thuengsuk, K Ruangjirakit, P Jongpradist and S Kongwat; Investigation, K Ruangjirakit, P Jongpradist and S Kongwat; Writing - original draft, P Noykanna, T Thuengsuk and T Homsnit; Writing - review & editing, K Ruangjirakit, P Jongpradist, S Kongwat and T Homsnit; Funding acquisition, K Ruangjirakit, P Jongpradist and S Kongwat; Resources, P Noykanna, T Thuengsuk and T Homsnit; Supervision, K Ruangjirakit, P Jongpradist and S Kongwat.

Editor: Pablo Andrés Muñoz Rojas

References

Akangah, P., & Shivakumar, K. (2013). Assessment of impact damage resistance and tolerance of polymer nanofiber interleaved composite laminates. Journal of Chemical Science and Technology, 2(2), 39-52.

Ary, A. K., Sanjaya, Y., Prabowo, A. R., Imaduddin, F., Nordin, N. A. B., Istanto, I., & Cho, J. H. (2021). Numerical estimation of the torsional stiffness characteristics on urban Shell Eco-Marathon (SEM) vehicle design. Curved and Layered Structures, 8(1), 167-180.

Cavazzuti, M., Baldini, A., Bertocchi, E., Costi, D., Torricelli, E., & Moruzzi, P. (2011). High performance automotive chassis design: a topology optimization based approach. Structural and Multidisciplinary Optimization, 44(1), 45-56.

Chen, H., Yang, Y., & Wang, L. (2015). Vehicle front structure energy absorbing optimization in frontal impact. The Open Mechanical Engineering Journal, 9(1).

Ciampaglia, A., Santini, A., & Belingardi, G. (2021). Design and analysis of automotive lightweight materials suspension based on finite element analysis. Proceedings of the Institution of Mechanical Engineers, Part C: Journal of Mechanical Engineering Science, 235(9), 1501-1511.

Czerwinski, F. (2021). Current Trends in Automotive Lightweighting Strategies and Materials. Materials, 14(21), 6631.

Denny, J., Veale, K., Adali, S., & Leverone, F. (2018). Conceptual design and numerical validation of a composite monocoque solar passenger vehicle chassis. Engineering Science and Technology, an International Journal, 21(5), 1067-1077.

Ewert, A., Brost, M., Eisenmann, C., & Stieler, S. (2020). Small and light electric vehicles: An analysis of feasible transport impacts and opportunities for improved urban land use. Sustainability, 12(19), 8098.

Fang, D., & Kefei, W. (2019). Simulation analysis and experimental verification on body-in-white static stiffness of a certain commercial vehicle. Vibroengineering Procedia, 29, 141-147.

Gheorghe, V., Scutaru, M. L., Ungureanu, V. B., Chircan, E., & Ulea, M. (2021). New design of composite structures used in automotive engineering. Symmetry, 13(3), 383.

Groenwold, A. A., & Haftka, R. T. (2006). Optimization with non-homogeneous failure criteria like Tsai–Wu for composite laminates. Structural and Multidisciplinary Optimization, 32(3), 183-190.

Hiller, M. (2020). Design of a Carbon Fiber Composite Monocoque Chassis for a Formula Style Vehicle.

Hoff, N. J. (1986). Monocoque, Sandwich and Composite Aerospace Structures: Selected Papers of Nicholas J. Hoff. (Book). Technomic Publishing Co., Inc., 1986.

Jongpradist, P., Saingam, N., Tangthamsathit, P., Chanpaibool, P., Sirichantra, J., & Aimmanee, S. (2022). Crashworthiness analysis and design of a sandwich composite electric bus structure under full frontal impact. Heliyon, 8(12), e11999.

Kim, S. I., Kang, S. W., Yi, Y. S., Park, J., & Kim, Y. Y. (2018). Topology optimization of vehicle rear suspension mechanisms. International Journal for Numerical Methods in Engineering, 113(8), 1412-1433.

Kongwat, S., & Hasegawa, H. (2020). New weight filtering factor of nonlinear design for topology optimization under cyclic loading based on proportional technique. Journal of Mechanical Science and Technology, 34(4), 1635-1644.

Kongwat, S., Homsnit, T., Padungtree, C., Tonitiwong, N., Jongpradist, P., & Jongpradist, P. (2022). Safety Assessment and Crash Compatibility of Heavy Quadricycle under Frontal Impact Collisions. Sustainability, 14(20), 13458.

Kongwat, S., Jaroenjittakam, S., Chaianan, S., Atchariyauthen, I., & Jongpradist, P. (2021). Design for crash safety of electric heavy quadricycle structure. Paper presented at the IOP Conference Series: Materials Science and Engineering.

Kongwat, S., Jongpradist, P., & Hasegawa, H. (2020). Lightweight bus body design and optimization for rollover crashworthiness. International journal of automotive technology, 21(4), 981-991.

Kunakorn-ong, P., & Jongpradist, P. (2020). Optimisation of bus superstructure for rollover safety according to ECE-R66. International journal of automotive technology, 21(1), 215-225.

Kunakorn-ong, P., Ruangjirakit, K., Jongpradist, P., Aimmanee, S., & Laoonual, Y. (2020). Design and optimization of electric bus monocoque structure consisting of composite materials. Proceedings of the Institution of Mechanical Engineers, Part C: Journal of Mechanical Engineering Science, 234(20), 4069-4086.

Li, S., & Feng, X. (2020). Study of structural optimization design on a certain vehicle body-in-white based on static performance and modal analysis. Mechanical Systems and Signal Processing, 135, 106405.

Malen, D. E. (2011). Fundamentals of automobile body structure design.

Messana, A., Sisca, L., Ferraris, A., Airale, A. G., de Carvalho Pinheiro, H., Sanfilippo, P., & Carello, M. (2019). From design to manufacture of a carbon fiber monocoque for a three-wheeler vehicle prototype. Materials, 12(3), 332.

Meyers, R. A. (2002). Encyclopedia of physical science and technology: Academic.

Pajot, J. (2013). Optimal design exploration using global response surface method: rail crush. Altair Engineering.

Patel, M., Pardhi, B., Chopara, S., & Pal, M. (2018). Lightweight composite materials for automotive-a review. Carbon, 1(2500), 151.

Patel, N. M., Kang, B.-S., Renaud, J. E., & Tovar, A. (2009). Crashworthiness design using topology optimization.

Reddy, I., Anjaneyulu, B., & Rao, K. (2016). Design and analysis of semi monocoque used sandwich composite beam. International Journal for Research in Applied Science and Engineering Technology, 4(12), 597-602.

Redelbach, M., Özdemir, E. D., & Friedrich, H. E. (2014). Optimizing battery sizes of plug-in hybrid and extended range electric vehicles for different user types. Energy policy, 73, 158-168.

Santa Rao, K., Musalaiah, G., & Chowdary, K. M. K. (2016). Finite element analysis of a four wheeler automobile car chassis. Indian Journal of Science and Technology, 9(2), 2-6.

Singh, R. P. (2010). Structural performance analysis of formula SAE car. Jurnal Mekanikal.

Sinha, K., Klimmek, T., Schulze, M., & Handojo, V. (2021). Loads analysis and structural optimization of a high aspect ratio, composite wing aircraft. CEAS Aeronautical Journal, 12(2), 233-243.

Story, R. D. (2014). Design of composite sandwich panels for a Formula SAE monocoque chassis. Corvallis: Oregon State University.

Sudin, M. N., Tahir, M. M., Ramli, F. R., & Shamsuddin, S. A. (2014). Topology optimization in automotive brake pedal redesign. International Journal of Engineering and Technology (IJET), 6(1), 398-402.

Tranchard, P., Samyn, F., Duquesne, S., Thomas, M., Estebe, B., Montès, J.-L., & Bourbigot, S. (2015). Fire behaviour of carbon fibre epoxy composite for aircraft: Novel test bench and experimental study. Journal of Fire Sciences, 33(3), 247-266.

Ugale, V., Singh, K., Mishra, N., & Kumar, P. (2013). Experimental studies on thin sandwich panels under impact and static loading. Journal of Reinforced Plastics and Composites, 32(6), 420-434.

Velea, M. N., Wennhage, P., & Zenkert, D. (2014). Multi-objective optimisation of vehicle bodies made of FRP sandwich structures. Composite Structures, 111, 75-84.

Wu, J., Badu, O. A., Tai, Y., & George, A. R. (2014). Design, analysis, and simulation of an automotive carbon fiber monocoque chassis. SAE International Journal of Passenger Cars-Mechanical Systems, 7, 838-861.

Wüstenhagen, S., Beckert, P., Lange, O., & Franze, A. (2021). Light Electric Vehicles for Muscle–Battery Electric Mobility in Circular Economy: A Comprehensive Study. Sustainability, 13(24), 13793.